doi:10.1016/j.jmb.2007.03.028 J. Mol. Biol. (2007) 369, 1015–1028

JMB

Available online at www.sciencedirect.com

ScienceDirect

ELSEVIER

A Designed Ankyrin Repeat Protein Evolved to Picomolar Affinity to Her2

Christian Zahnd[1]†, Emanuel Wyler[1]†, Jochen M. Schwenk[2] Daniel Steiner[1], Michael C. Lawrence[3], Neil M. McKern[3] Frédéric Pecorari[1], Colin W. Ward[3], Thomas O. Joos[2] and Andreas Plückthun[1]*

[1]*Biochemisches Institut der Universität Zürich Winterthurerstr. 190 CH-8057 Zürich, Switzerland*

[2]*NMI Naturwissenschaftliches und Medizinisches Institut an der Universität Tübingen Markwiesenstr. 55, D-72770 Reutlingen, Germany*

[3]*CSIRO, Molecular and Health Technologies 343 Royal Parade, Parkville Victoria 3052, Australia*

**Corresponding author*

Designed ankyrin repeat proteins (DARPins) are a novel class of binding molecules, which can be selected to recognize specifically a wide variety of target proteins. DARPins were previously selected against human epidermal growth factor receptor 2 (Her2) with low nanomolar affinities. We describe here their affinity maturation by error-prone PCR and ribosome display yielding clones with zero to seven (average 2.5) amino acid substitutions in framework positions. The DARPin with highest affinity (90 pM) carried four mutations at framework positions, leading to a 3000-fold affinity increase compared to the consensus framework variant, mainly coming from a 500-fold increase of the on-rate. This DARPin was found to be highly sensitive in detecting Her2 in human carcinoma extracts. We have determined the crystal structure of this DARPin at 1.7 Å, and found that a His to Tyr mutation at the framework position 52 alters the inter-repeat H-bonding pattern and causes a significant conformational change in the relative disposition of the repeat subdomains. These changes are thought to be the reason for the enhanced on-rate of the mutated DARPin. The DARPin not bearing the residue 52 mutation has an unusually slow on-rate, suggesting that binding occurred *via* conformational selection of a relatively rare state, which was stabilized by this His52Tyr mutation, increasing the on-rate again to typical values. An analysis of the structural location of the framework mutations suggests that randomization of some framework residues either by error-prone PCR or by design in a future library could increase affinities and the target binding spectrum.

Keywords: ErbB2/Her2; designed ankyrin repeat protein (DARP)in; *in vitro* selection; ribosome display

Introduction

Antibodies with high affinity to disease-relevant antigens, such as tumor markers or chemokines, have been widely investigated for their use in therapy and diagnostics. Antibody engineering techniques have facilitated the generation of high affinity protein binders for targeted therapy.[1,2] The introduction of antibody-fragments and novel selection methods such as phage display or ribosome display has allowed the fast isolation of specific binding proteins from vast synthetic libraries *in vitro*.[3,4] Selections from such libraries have been shown to routinely yield specific binders, with the

† C.Z. and E.W. contributed equally to this work.

Present addresses: C. Zahnd, Molecular Partners AG, Grabenstrasse 11a, CH-8952 Schlieren, Switzerland; E. Wyler, Institute of Biochemistry, ETH Zürich, CH-8093 Zürich, Switzerland; F. Pecorari, Unité de Biochimie Structurale – CNRS URA 2185, Institut Pasteur, 25 rue du Dr Roux, 75724 Paris Cedex 15, France.

Abbreviations used: ECD, extracellular domain; IHC, immunohistochemistry; RIA, radioimmuno assay; RMS, root mean square; SPR, surface plasmon resonance.

E-mail address of the corresponding author: plueckthun@bioc.unizh.ch

0022-2836/$ - see front matter

highest affinity binders typically being in the low nanomolar affinity-range.

For therapeutic and diagnostic applications, particularly against cell-surface targets, the retention time on the target is usually a crucial factor limiting the efficacy of the antibody reagent.[5] Affinity maturation of binders is therefore considered to be an important means to improve the properties of previously selected binders, and the selection for slower dissociation-rates with competitive off-rate selections has proved to be a powerful method for improving affinity.[6,7] This strategy is based on the observation that, usually, the on-rates for forming protein–protein interactions fall into a narrow window[8] and affinity is thus normally correlated with off-rate. Such evolved high-affinity antibodies have been used with great success in many applications.[2]

An alternative, novel approach to developing high-affinity binding reagents takes advantage of another natural class of binding proteins, termed ankyrin repeat proteins.[8] Ankyrin repeat proteins are built from a single structural motif, which is assembled into a protein domain. Due to the relatively high sequence homology within these ankyrin repeats, a consensus sequence module could be deduced from the natural ankyrin repeat proteins, identifying putative structure-determining framework residues (i.e. residues which on the basis of sequence conservation appear to be important for maintaining the repeat structure) and interaction-mediating binding residues.[9,10] A synthetic consensus repeat module of the ankyrin repeat protein family could be assembled into complex libraries of designed ankyrin repeat proteins (DARPins), from which binding proteins could be isolated that showed exceptional expression yields, stabilities[9,11] and affinities in the low nanomolar range.[11] Due to the modularity of the design, DARPins with more binding modules and consequently larger binding interfaces are feasible and a stepwise enlargement of the binding interface could even be considered as a way of affinity maturation. The exceptional stability and folding efficiency of DARPins might also allow novel therapeutic approaches such as potent DARPin-toxin fusions or bivalent DARPin constructs.

Epidermal growth factor receptor 2 (Her2) is a cell surface receptor, which has been shown to be over-expressed in several cancer tissues, including breast and colon carcinoma, and its over-expression has been linked to poorer prognosis of the patients. Only 20–30% of all breast cancer patients, however, show over-expression of Her2, making the determination of the state of the Her2 expression of a cancer patient an important diagnostic step in assessing the suitability of anti-Her2 therapy for the patient. Currently, one antibody against Her2 has been approved for the treatment of breast cancer and several other tumor types are in clinical trials.

In a previous study, DARPins binding to the extracellular domain of Her2 (Her2 ECD) with high specificity and low nanomolar affinities had been selected[12] from large synthetic libraries *in vitro* using ribosome display.[3] After six rounds of selection, several binders with nanomolar affinities were obtained and characterized. They were shown to bind the cognate antigen both as a purified protein and on different Her2-overexpressing cell lines and *in situ* in tissue sections of Her2-positive mammary carcinomas. For both therapeutic and diagnostic applications, the affinity of the Her-2 binding molecule is expected to be crucial. Therefore, Her2 is an ideal model system to explore the potential for affinity maturation of DARPins.

Here, we aimed to explore the affinity limits obtainable for DARPins by subsequent randomization of the selected pools in combination with *in vitro* selection under very stringent conditions, and particularly to investigate the structural consequences of affinity maturation in this scaffold.

For the present study we used rather small DARPin molecules containing only two randomized repeat modules (termed N2C). These N2C DARPins display an interaction surface that is smaller than the average interaction surface of an antibody. The small size of the DARPin, which should allow good tumor penetration, in combination with its high stability and expression yield, would provide the basis for the development of an *in vitro* and possibly also *in vivo* diagnostic test for the expression state of Her2 in cancer tissues. We have characterized the binding properties of the affinity-matured DARPins, including their ability to detect Her2 in solubilized tumor tissue. In addition, we have determined the crystal structure of the N2C DARPin with the highest affinity, which has allowed us to demonstrate that the selected mutations cause a change in the positioning of the side-chain of the residue at position 52 and, as a consequence of this mutation, cause a significant conformational change in the relative disposition of the repeat domains in this structure compared with their counterparts in the previously determined structures. These structural changes are thought to be the cause of the enhanced on-rate of the mutated DARPin.

Results

DARPins had been selected from large synthetic libraries *in vitro* using ribosome display[3] and binders specific for Her2 with nanomolar affinities were obtained.[12] We wished to affinity-mature these binders for their potential application as diagnostics and therapeutics and characterize the biophysical and structural consequences of affinity maturation in this protein architecture.

Selection procedure

Analysis of the previously selected pools revealed that most binders belonged to only a few sequence families. To increase the diversity in these pools and to extend the randomization to framework po-

sitions, which were fixed in the original library design,[9] error-prone PCR was performed in the presence of dNTP analogs as described earlier.[6,13] Several new pools were generated using all previously isolated pools as a starting point. The average mutation rate in the different reactions (with different mutation rates) was determined by sequencing to be 1.3–5.9 mutations per gene. For the following selection, the libraries with different mutation rates were combined.

The pools obtained were converted into the ribosome display format and subjected to three rounds of off-rate selection.[6] The selection pressure is mainly defined by the incubation time of the pools in the presence of a large molar excess of competitor antigen. It was increased from round to round, from 10 h initially to 100 h in the second round. In the third selection round, a first aliquot was isolated after five days and a second after 25 days. It has been shown that after very stringent off-rate selections, the fraction of remaining binders is very low compared to non-binding background clones.[7] This fraction can be increased by applying an additional selection round at low stringency, thereby enriching the diluted binders. Thus an additional panning round with no additional selection pressure was applied. The percentage increase in the binder clones after this non-selective selection round could be monitored by radioimmuno assay of the pools, resulting in a fivefold increase of the binding signal (data not shown). In addition, after cloning of the pools in an expression vector in *E. coli*, crude extract ELISA of single clones also indicated that there was an increase in specific binding clones. After the last off-rate selection round, five out of 92 analyzed clones (5%) showed specific binding. After the additional non-selective panning round, this ratio increased to 68 out of 92 (74%).

Sequences of binders

Those binders giving a specific binding signal in a crude extract ELISA were sequenced. Four major sequence families were found in the selected pool. According to the amino acid sequence in the first four randomized positions, the sequence families were termed the LWRF, the LWRL, the KEYL and the KWIF family. Representative sequences of binders are shown in Figure 1, kinetic parameters from BIAcore measurements are shown in Table 1 and Figure 2. Interestingly, an N1C DARPin showing target binding was also isolated, which might have been generated by recombination from an N2C DARPin gene.

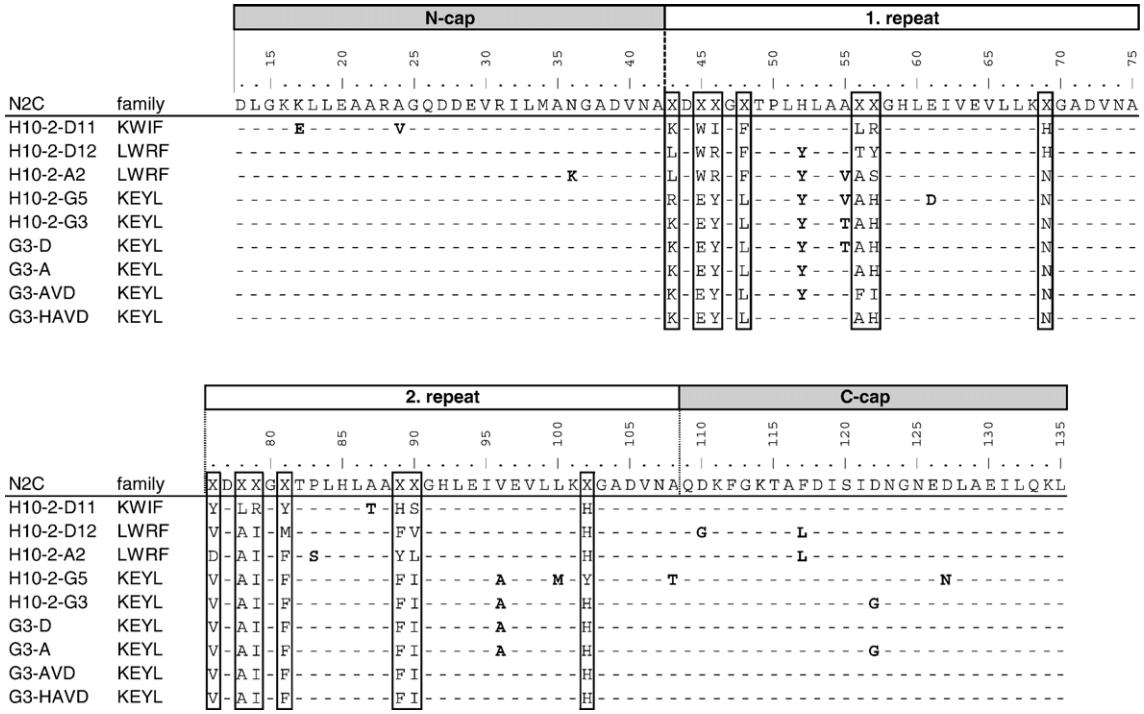

Figure 1. Sequences of selected DARPins and framework mutants of H10-2-G3. The sequences of different DARPins are shown. Randomized positions in the N2C family sequence (first line) are indicated by X. In the lower lines, only residues that differ from the consensus sequence of an N2C DARPin are printed. Residues that had been randomized in the original design are boxed. Mutations that showed up at framework positions (outside the boxes) are printed in bold. Four major sequence families were found after affinity maturation, termed KEYL, KWIF, LWRL and LWRF, according to the first randomized positions in the first module. The respective sequence family is also indicated. The clone with the highest affinity found was H10-2-G3. It contained four framework mutations (at residues 52, 55, 96 and 122) in addition to those residues that had been randomized by design. To investigate the effect of the different framework mutations, several mutants of this clone were constructed, turning the sequence back to the consensus sequence. These clones are listed in the lower part.

Table 1. Kinetic parameters of the binding of different DARPins

Clone name	Sequence family	K_D/nM	$k_{on}/10^4$ $M^{-1}s^{-1}$	$k_{off}/10^{-3}s^{-1}$
H10-2-G3	KEYL	0.091±0.001	112.3±0.19	0.102±0.001
G3-D	KEYL	1.48±0.008	76.8±0.36	1.14±0.002
G3-A	KEYL	1.21±0.006	61.8±0.26	0.745±0.002
G3-AVD	KEYL	10.2±0.055	43.5±0.22	4.42±0.008
G3-HAVD	KEYL	269±1.19	0.275±0.001	0.739±0.003
H10-2-G5	KEYL	0.670±0.005	26.6±0.036	0.178±0.001
H10-2-D11	KWIF	35.8±0.149	15.4±0.057	5.52±0.011
H10-2-D12	LWRF	93.9±1.12	30.5±0.31	28.6±0.17
H10-2-A2	LWRF	3.46±0.017	11.9±0.019	0.411±0.002

The statistical errors in the parameters given are those obtained from the best fit error.

As described below, the binder with the highest affinity, H10-2-G3 (KEYL family) has a picomolar affinity to the target. The K_D is about one order of magnitude better compared to the second best binder analyzed from the KEYL family. Interestingly, despite its high affinity, clone H10-2-G3 was only found once out of 68 sequenced clones. Only six out of the 68 analyzed clones belonged to the KEYL family. This indicates that high affinity is either not the only important factor for survival in the applied selection system or that the enrichment for high affinities has not yet reached its limit.

Compared to the sequences found in the selected pools prior to error-prone PCR, many mutations were found at so-called framework positions[9] as a consequence of the applied randomization. The average number of amino acid substitutions at framework positions was about 2.5 per sequence, ranging from several clones having no framework mutation, up to seven amino acid substitutions at framework positions per gene. It is likely that variable positions had also been randomized during error-prone PCR. This would not be detectable in the final sequence, although the actual number of mutations in the selected clones was increased.

The same sequence families that were present before off-rate selection could also be found after off-rate selection. However, the relative abundance of the different sequence families had changed. Whereas about 50% of the binders found before off-rate selection belonged to the KWIF-family, only 14% of the binders found after error-prone PCR and off-rate selections were of the KWIF-type. The LWRL-family, which finally contributed 28% of all binders, had not been found before off-rate selection.

Compared to previously described selection experiments against other targets, such as maltose binding protein and MAP kinases,[11] it was striking that most of the randomized variable positions in the selected Her2 ECD binders were hydrophobic. Up to 11 out of 14 variable residues were either aromatic or aliphatic amino acids. Ten of these built up an extended hydrophobic patch on the binding interface of the ankyrin repeat protein in the most extreme case. Since the interaction interface of the chosen DARPin library (consisting of only two ankyrin repeats) was limited in size, this might have been the only molecular solution to generate binders with affinities high enough to survive the selection pressure. However, despite the relatively large contiguous hydrophobic surface of the selected binders, no non-specific binding was observed (see below).

Affinities of Her2 binders

Based on the binding signals obtained in crude extract ELISA and the competition behavior with free Her2 ECD, several clones were chosen for expression, purification, affinity determination and further analysis. For each sequence family, several DARPins were expressed in the *Escherichia coli* strain XL1-blue. Despite the framework mutations, expression yields were similarly high as found previously[9,11] and also similar among the various clones, corroborating the robustness of the framework to also carry high mutational loads outside the randomized positions. The clones were purified to 95% purity *via* IMAC, and affinities were determined using kinetic and equilibrium surface plasmon resonance (SPR) measurements.

To get an initial affinity ranking, all expressed and purified clones were injected at a single concentration and the most promising binders were chosen for detailed measurements. Affinities were determined by kinetic SPR measurements with protein samples having any minor potential non-monomeric fractions removed by preparative gel filtration. The dissociation constants K_D of the measured affinities were found to be between 91 pM and 94 nM (Table 1). The binder with the highest affinity, termed H10-2-G3, was measured several times independently with different protein preparations and both kinetic and equilibrium measurements.[14–16] The kinetic measurements revealed an association rate constant of 1.1×10^6 $M^{-1}s^{-1}$ and a dissociation rate constant of 1.0×10^{-4} s^{-1}, giving rise to an equilibrium dissociation constant of 90 pM. Equilibrium measurements of the dissociation constant resulted in a K_D of 91 pM (Figure 2).

Clone H10-2-G5 (K_D of 670 pM) differed mainly at framework positions from H10-2-G3 (six differences), but had very similar amino acids at the variable positions (only two residues differ at positions 43 and 102; Figure 1). Although they belong to the same sequence family, their affinities differ by one order of magnitude. Most other binders showed affinities in the low nanomolar range (Table 1).

In the non-affinity-matured pools (starting material for this study), the clone with the highest affinity, termed H6-2-A7, had an affinity of 7.3 nM,[12] which is 80-fold lower than the affinity shown by H10-2-G3. Interestingly, clone H6-2-A7 had the same amino acid sequence in the first variable module as H10-2-G3, but a completely different sequence in the second variable module.

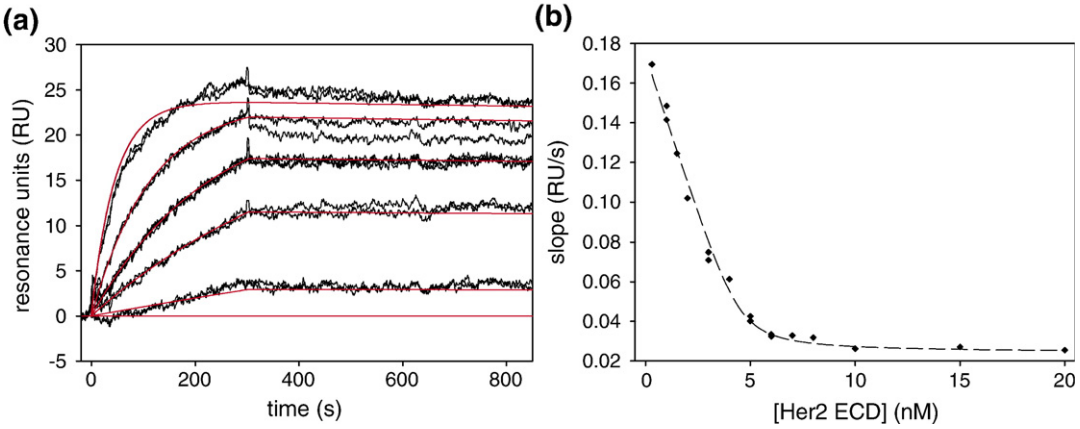

Figure 2. Affinity determination of clone H10-2-G3 using SPR. (a) The kinetics of binding of clone H10-2-G3 to Her2 ECD was monitored using Biacore. Her2 ECD was immobilized on a flow cell at low concentrations. Binding of the DARPin to the immobilized target protein was compared to binding to an empty flow cell at increasing concentrations of the DARPin (1 nM, 5 nM, 10 nM, 20 nM, 30 nM). The data were evaluated using global fitting with the software CLAMP.[26] The predicted curves are drawn in red. (b) The affinity was also determined at equilibrium using competition Biacore. The affinity values obtained by both methods were consistent.

Influences of framework mutations on affinity

The use of error-prone PCR allowed the introduction of framework mutations. However, in earlier selection rounds, several framework mutations already had become enriched. This intrinsic randomization of pools that are selected by ribosome display has been described before.[16] At position 52, the framework mutation histidine to tyrosine (H52Y) was found in 86% of all binders. Even before error-prone PCR, this mutation was found in some members of the KEYL-sequence family, suggesting that this mutation evolved independently several times.[12] Since this mutation has not been found in any of the other selection experiments performed with DARPins, we concluded that this mutation would be important for binding to the target Her2.

To test the influence of the observed framework mutations on the affinity of H10-2-G3, several mutants were constructed restoring the original framework residues (Figure 1). The four framework mutations found in H10-2-G3 were: H52Y and A55T, both residing in the first variable repeat module, V96A in the second variable repeat module and D122G in the C-terminal capping repeat. We generated four clones, the first termed G3-D, lacking the D122G mutation, the second termed G3-A, lacking the A55T mutation, the third G3-AVD without the mutations A55T, V96A and D122G and finally clone G3-HAVD, which corresponds to

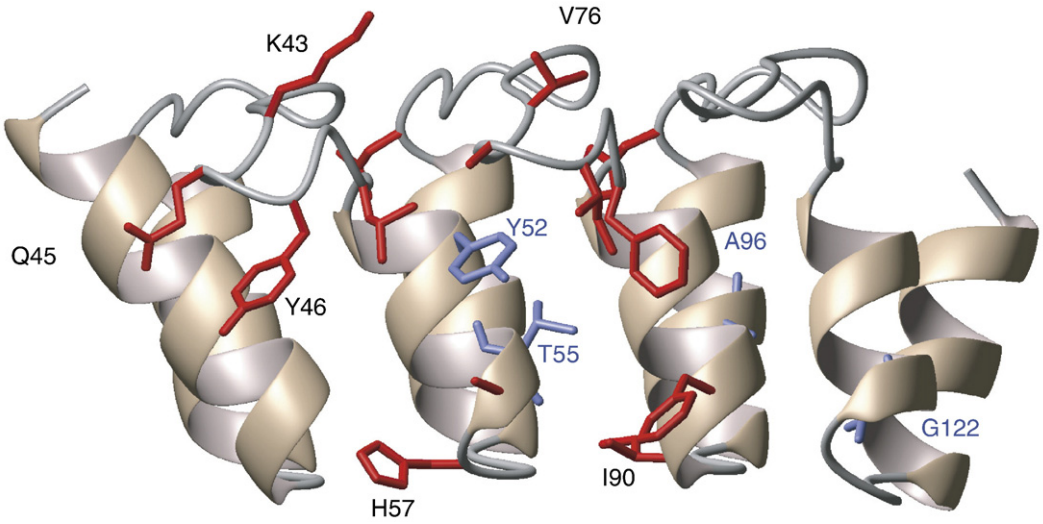

Figure 3. Crystal structure of H10-2-G3. The overall structure is shown in ribbon representation in front view, looking towards the putative binding surface. The side-chains of residues that had been randomized in the synthetic library are drawn in red. Side-chains of framework residues that had been mutated in the course of affinity maturation are drawn in blue. Note that only some of the side-chains that have been drawn are labeled.

H10-2-G3 with the original DARPin framework. All clones were expressed and purified and affinities were determined using kinetic SPR (Supplementary Data Figure).

All back-mutated clones had lower binding affinities than clone H10-2-G3 (Table 1). The reversion of the single mutations A55T and D122G had similar effects on the equilibrium dissociation constant, decreasing the affinity by about 15-fold each. The reversion of the triple mutation in G3-AVD reduced the affinity by over 100-fold, while the reversion of the additional mutation H52Y lead to a further 26-fold decreased affinity (compare G3-AVD with G3-HAVD) and an about 3000-fold decreased affinity compared to H10-2-G3. Interestingly, reversion of the mutation H52Y influenced mostly the on-rate, and since the off-rate changes much less, the affinity is lowered by about two orders of magnitude in the mutant.

The major contribution to the improved affinity obtained by the evolutionary approach was thus due to an increase in the association rate constant of the binding. This was not expected, since the association rate constant is usually governed by translational diffusion and orientation-dependent collisions, at least in solutions of moderate or high ionic strength. Therefore, it tends to be rather similar in most protein–protein interactions. For interacting proteins with molecular masses similar to the present example, association constants of 10^5–10^6 s^{-1} M^{-1} would be expected, if the process was diffusion-controlled.[8] The association rate constant of H10-2-G3 was determined to be 1.1×10^6 s^{-1} M^{-1}, which is in the expected range. For most of the non-affinity matured binders, the association rate constant was two to tenfold lower. However, in the quadruple "back"-mutant of the KEYL family, G3-HAVD, k_{on} was dramatically reduced (400-fold, compared to H10-2-G3 and 160-fold compared to G3-AVD, which differs only by carrying His52 instead of Tyr52). This strongly indicates that there is a rate-limiting step in the formation of the DARPin Her2-ECD complex other than simple diffusion. This could either be due to slowly forming structural rearrangements that have to occur prior to binding or be due to rapidly equilibrating conformations, of which an only sparsely populated one is able to bind. In the other protein families (KWIF and LWRF), the H52Y mutation does not correlate with k_{on}, suggesting that this effect is connected to the epitope recognized by the members of the KEYL-family (see below).

It should also be noted that most of the framework mutations are not at the putative binding site of the DARPin. While D122G could be involved in binding, and maybe also H52Y, mutations A55T and V96A are most likely not part of the binding interface, based on their location (see Figure 3). The differences between H10-2-G3 and H10-2-G5 (Figure 1) involve amino acid residues that are part of the hydrophobic core or reside on the back of the DARPin, except for K43R. Possible explanations for these observations are detailed in Discussion.

Crystal structure of H10-2-G3

To further analyze the influence of framework mutations on the binding kinetics, the crystal structure of the clone H10-2-G3 was determined to a final resolution of 1.7 Å, an *R*-value of 17.8% and an R_{free} of 21.2% (Table 2). The structure solution with three molecules of H10-2-G3 found in the crystallographic asymmetric unit was achieved *via* molecular replacement. The overall backbone of H10-2-G3 (Figure 3) was similar to the previously determined structures of DARPins,[11,12,19] with an overall root mean square (RMS) displacement of the backbone atoms of 1.13 Å compared to the N2C model.

However, there are two striking differences compared to representative N3C structures. The first is a rotameric[17] change at position 52 in conformation of the side-chain from *m*80° if it is occupied by histidine to *t*80° if it is occupied by Tyr in H10-2-G3. This mutation causes a change in the inter-repeat disposition (see below). H10-2-G3 has four mutations in the designed framework, H52Y, A55T, V96A and D122G. After testing the influence of all four mutations on the binding affinity (see above), mutation H52Y was shown to have the most substantial influence on the on-rate and its structural consequences were therefore analyzed in detail. This mutation, as well as D122G, is located on the side of the DARPin potentially facing the target, while the other two mutations are buried inside the molecule.

Analysis of the crystal structures of unselected N3C DARPins[18] reveals that the histidine at position 52 participates in an extended hydrogen bond network: His52 $N^{\delta1}$ to Thr49 $O^{\gamma1}$ and His52 $N^{\varepsilon2}$ to the carbonyl oxygen of residue 81 (Figure 4(a)). These inter-repeat unit hydrogen bonds likely contribute to the known extraordinary stability of DARPins (see below). However, the H52Y mutation and the concomitant rotameric change at that position causes a loss of both these hydrogen bonds, replacing them with a single hydrogen bond between Tyr52 O^{η} and Asp77 $O^{\delta2}$ (Figure 4(b)). No disruption is caused to the hydrogen-bonding pattern within the α-helical backbone at that mutation site. Rotameric rearrangement of the side-chain

Table 2. X-ray data collection and processing statistics

	Data set 1	Data set 2
Detector 2θ (°)	0	15
Resolution range (Å)	∞–2.00 (2.03–2.00)	∞–1.70 (1.73–1.70)
No. of frames	200	310
Oscillation range (°)	1	1
No. of measurements	144,477	225,321
No. of reflections	35,218	58,105
Redundancy	4.1 (3.7)	3.8 (2.4)
Completeness (%)	97.7 (94.6)	98.6 (93.3)
R_{merge}[a]	0.11 (>1.0)	0.12 (0.88)
$\langle I\rangle/\langle\sigma\rangle$	15.5 (1.6)	13.2 (1.3)

Numbers in parentheses refer to the statistics for the outer resolution shell.

[a] $R_{merge}=\sum_h\sum_i|\langle I_h\rangle-I_{h,i}|/\sum_h|\langle I_h\rangle|$.

at Leu86 is also evident, presumably to relieve steric clash with the Tyr52 side-chain. The second, more dramatic difference is that the positioning of the phenol ring of Tyr52 in the groove formed by the first helices of the two randomized repeats necessitates an opening-up of the N2C structure with respect to its unmutated counterparts (Figure 4(c)), effected by an $\omega = 13(\pm 1)°$ rotation of the second randomized and C-cap repeat (grouped as a single domain) with respect to the N-cap and first randomized repeat (grouped as a single domain). The hinge point of this rotation lies in the vicinity of residue 76. Whilst the size of ω and the direction of the rotation axis are closely similar for all pairwise N2C-to-N3C comparisons conducted here, the spatial location of the rotation axis itself is somewhat ill-defined, a mathematical consequence of ω being small. The relative rotation of the N and C-terminal halves of the N2C structure results in the loss of the hydrogen bond between the backbone carbonyl at position 46 and the backbone amide at position 78, the respective O and N atoms of these residues now being about 6 Å apart (Figure 4(a) and (b)).

Since all clones of the KEYL family having this H52Y mutation had an association rate constant that was increased by up to two orders of magnitude to reach values expected for protein–protein interactions (see above), the importance of this residue on the overall structure of the DARPin may not surprise. It is in principle possible that Tyr52 directly interacts with Her2 ECD, but we have no evidence for or against this. It is likely that the "opened-up" structure is the one that interacts optimally with the target. The original framework could adopt, as a sparsely populated state, an overall conformation that is similar to the conformation found with Tyr52. Such a break-up of the repeats could even allow His52 to adopt a similar rotameric conformation as seen here for Tyr52 (i.e. directed away from the N2C structure and towards the target), but this does not imply productive interaction of His52 with the target. A similar interaction of Tyr and His with the target would be difficult to conceive because of the different side-chain characteristics. If binding occurs by conformational selection, i.e. if only a minor fraction of the binding molecules is in the reactive "open" conformation, the bimolecular binding reaction would appear to be slow. Note that this effect would not affect the off-rate. The mutation H52Y most likely stabilizes the outward rotated conformation and thereby increases the active concentration of the binder, giving rise to a "normal" on-rate. In addition, the other mutations might optimize existing interactions or introduce new ones. The change in the overall conformation might assist adaptation to the antigen.

Note that the change in on-rate, interpreted as a conformational selection that gets stabilized by mutation, is a phenomenon only found in the KEYL family. In the other families, completely normal rates of association are found, despite the fact that they all contain His52. We interpret this as indicating a necessity for an open conformation only for binding to the epitope of the KEYL family, but clearly not a general phenomenon of DARPins. Consistent with this view, all association rates measured with binders to other targets fell in the usual windows, and all crystal structures determined so far[11,12,19] indicated a consensus spacing of repeats.

Conformational variability or even partial unfolding can be an important parameter controlling interactions of some natural ankyrin repeat proteins,[21–24] whereas other natural ankyrin repeat proteins[19] have been shown to be very stable and display two-state folding. The consensus-designed DARPins have previously been shown to be particularly stable.[9] We were thus interested in determining whether the His52Tyr mutation had an effect on the thermal stability of H10-2-G3 and therefore measured it and compared it to that of the "restored" consensus framework variant, G3-HAVD. We found that G3-HAVD is significantly more stable than H10-2-G3: the mutations in the framework acquired in affinity maturation did indeed lead to a decrease of the midpoint of denaturation from 89.4(±0.6) °C to 69.1(±0.02) °C (Figure 5). For both proteins, H10-2-G3 and G3-HAVD, the measurement was performed with material that had been purified by gel filtration to remove any potential non-monomeric species. Furthermore, the protein had been analyzed by multi-angle light scattering (MALS) to verify its monomeric state. These MALS results exclude that the observed stability change was due to the presence of dimers of G3-HAVD. Neither of the two proteins showed significant dimeric fractions even at very high concentrations of more than 100 μM (data not shown).

Therefore, the conformational change caused by the introduction of these evolved framework mutations destabilizes the molecule, but not to the point of imparting any handling disadvantage on this evolved protein, as even the affinity-matured H10-2-G3 still has a stability in the upper range of typical globular proteins, and no difference in handling was noticed in purification or any treatment compared to other DARPins. In particular, the high soluble expression yield is fully maintained for the evolved DARPin. The consensus protein G3-HAVD, a typical member of the original library from which the directed evolution had presumably started, has such a high stability that the conformational changes and some ensuing loss of stability are easily tolerated. This high stability of the consensus-designed libraries is one of the key features ensuring that affinity maturation still leads to molecules with very favorable properties without further stability engineering.

A more complete analysis of the influence of the mutations could be obtained by the analysis of the binding interface in a co-crystal of Her2 and H10-2-G3. Presumably not only the randomized positions (those designed to be variable in the original library) participate in binding of the DARPin to its target, but also at least some of the selected framework positions, as shown, for example, by the considerably lower K_D of the G3-D mutant compared to H10-

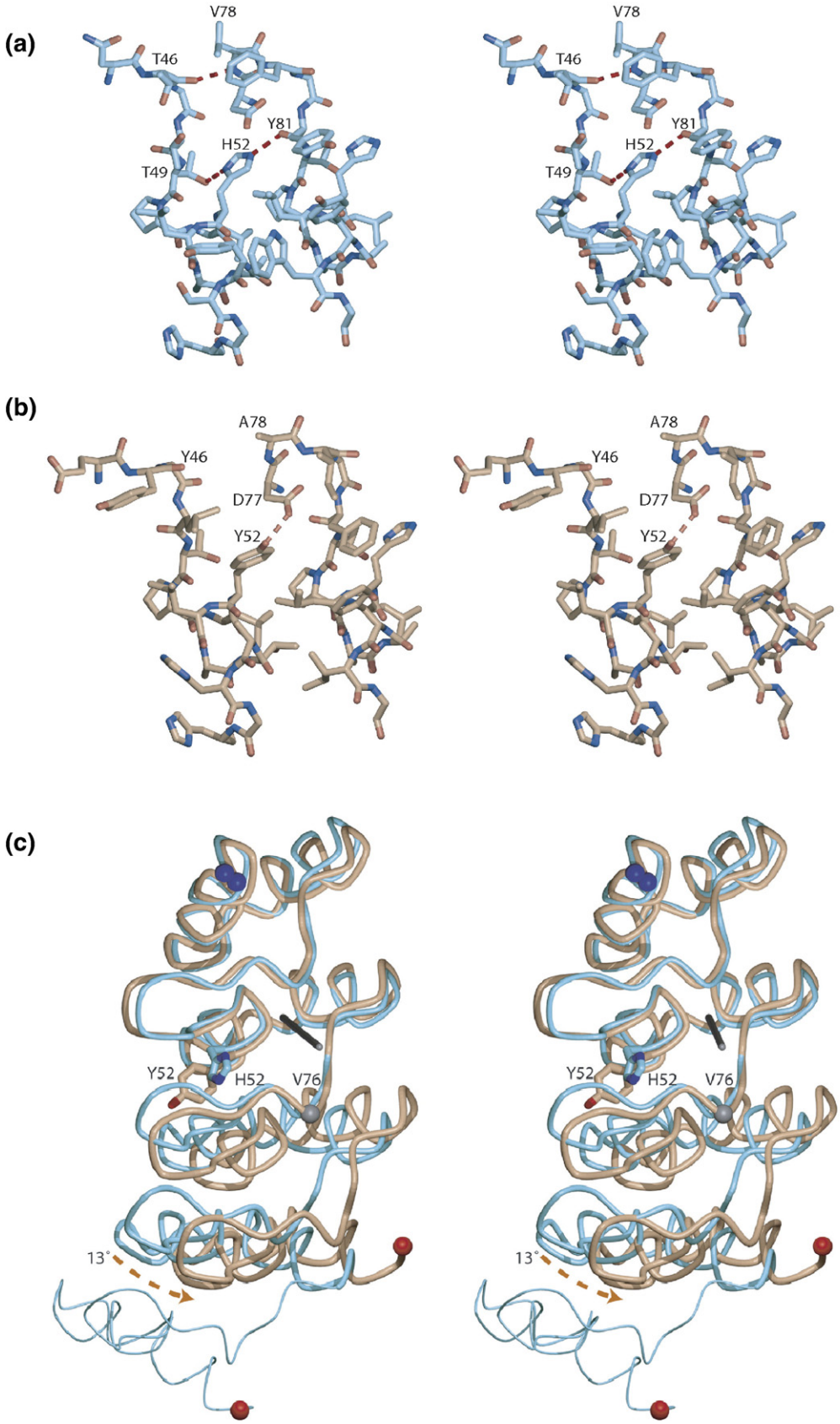

Figure 4 (*legend on next page*)

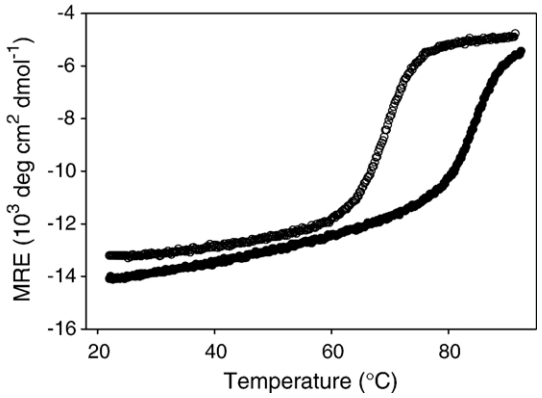

Figure 5. Thermal denaturation of H10-2-G3 (open circles) and G3-HAVD (filled circles), a variant of H10-2-G3 that carries no mutations at framework positions. Both proteins were heated from room temperature to 95 °C and the circular dichroism was measured at 222 nm. The midpoints of denaturation were estimated from extrapolation of the curves to be at 69 °C and 89 °C, respectively.

2-G3. The residue where G3-D differs, Gly122, is in the C-cap, and it could make a direct contact or the original interaction with Asp122 could have been unfavorable, even by indirect electrostatic effects. In a biochemical analysis and in the absence of a structure of a complex, however, it is difficult to distinguish between mutations that help the adaptation of the DARPin structure to the antigen epitope and mutations of amino acids that actually bind to the target.

Epitope characterization and specificity of affinity matured binders

DARPins selected before affinity maturation were shown to bind to different epitopes and some competed for the same epitope with trastuzumab (Herceptin™), an antibody used in therapy. We therefore tested if the binding of the affinity-matured DARPins could still be inhibited with antibodies. We assayed the selected clones with trastuzumab, which has been shown to bind to the membrane-adjacent cysteine-rich domain IV[20] and pertuzumab, another antibody under development for its use in therapy, which binds to domain II.[21] In competition ELISA, all binders of the KWIF-sequence family competed with trastuzumab for the epitope as shown previously for the non-affinity matured DARPins.[12] None of the selected and analyzed binders competed with pertuzumab for Her2 ECD (data not shown).

The highest affinity DARPins were investigated for their cross-reactivity with unrelated proteins, including epidermal growth factor receptor 1 (EGFR). As shown in the previous work for non-matured binders,[12] none of the affinity-matured binders showed non-specific binding (data not shown).

Sensitivity analysis of the selected DARPins

To evaluate the use of the selected and affinity-matured DARPins for the quantification of Her2 in sandwich immunoassays, we tested five binders (three representative ones are listed in Figure 6(a)) in a multiplexed format. For this purpose, the DARPins were expressed with N-terminally fused phage lambda protein D (pD) containing an avi-tag, to allow site-specific biotinylation with the *E. coli* biotin ligase BirA. Each of the biotinylated DARPins was immobilized on a different population of spectrally distinguishable avidin-coated Luminex microspheres. These beads were incubated with various concentrations of the recombinant ECD of Her2. After the binding step, detection was performed by either adding a second DARPin bearing a myc-tag or commercially available anti-Her2 antibodies to set up a sandwich assay. This method allowed a fast screening for the best combination of the five DARPins and three different commercially available murine monoclonal antibodies against Her2. Although several of the DARPin-DARPin combinations could be used in the sandwich format (data not shown), the best sandwich combination turned out to be when using a DARPin for capturing and the antibody sp185 for detection. This is most likely due to the fact that the investigated high-affinity DARPins do not make suitable sandwich pairs because they bind to the same or to nearby epitopes.

Large differences were seen when using the different DARPins as capture reagents in this assay

Figure 4. A stereo diagram showing detail of the accommodation of the imidazole ring of His52 in a representative N3C structure (PDB entry 1SVX) is shown in (a). Oxygen atoms are shown in red, nitrogen atoms in blue and carbon atoms in cyan. The hydrogen bonds between the imidazole ring of His52 and the respective atoms Thr49 $O^{\gamma 1}$ and Tyr81 O are indicated by broken red lines, as is the inter-repeat hydrogen bond between Thr46 O and Val78 N. (b) Stereo diagram showing detail of the accommodation of the phenol ring of Tyr52 in the N2C structure presented here. Oxygen atoms are shown in red, nitrogen atoms in blue and carbon atoms in copper. The single hydrogen bond between the side-chain hydroxyl of Tyr52 and the side-chain carboxylate of Asp77 is indicated by a broken red line. The increased separation (ca 6 Å) of the respective backbone atoms at positions 46 and 78 compared to the N3C structure shown in (a) is apparent. (c) Stereo diagram showing an overlay of the backbone traces of H10-2-G3 (copper) with an N3C structure (PDB entry 1SVX, cyan) generated by superimposing the C^{α} atoms of residues 12 to 74 of the two structures. The rotameric change at position 52 is indicated. The 13° relative rotation of the two C-terminal ankyrin repeats of H10-2-G3 with respect to their N3C counterparts is apparent, with the grey line showing the approximate location of the rotation axis and the sphere at residue 76 indicating the approximate point in the backbone trace at which the overlaid structures begin to diverge. The Figures were generated using Molmol[35] and POVScript+.[39]

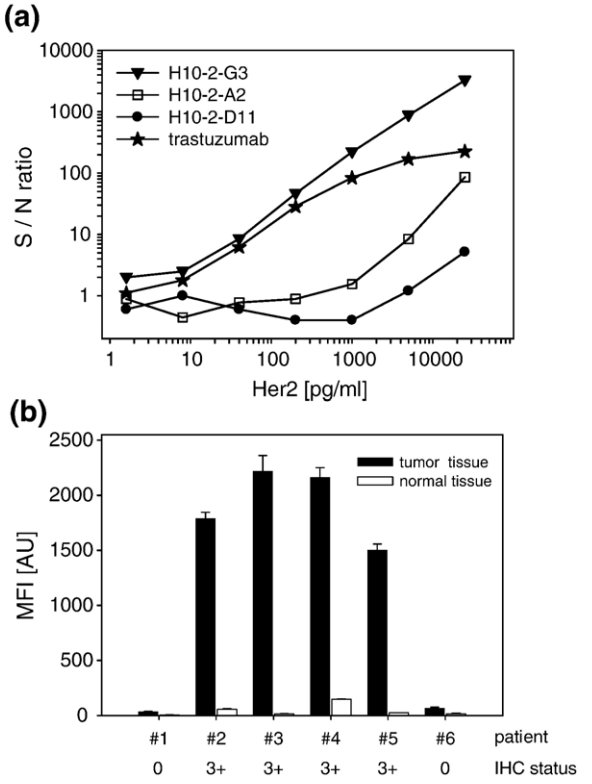

Figure 6. DARPins in immunoassays for Her2 detection. (a) The capture activities of three representative DARPins were compared in a sandwich immunoassay. These DARPins were biotinylated and site-specifically immobilized on Luminex microspheres. In a six-plex assay format including bead-coupled trastuzumab, capture activities were analyzed in a titration series of Her2 ECD. The monoclonal anti-Her2 antibody sp185 was applied for detection of bound Her2. The sensitivity of the DARPins appeared to correlate with the affinity. The ratio of signal over background (S/N: signal to noise ratio) was chosen to display qualitative differences of capture activities. (b) Clone H10-2-G3 was used as a capture reagent to detect Her2 from solubilized breast tissue of patient samples in a sandwich assay, with monoclonal antibody sp185 as detection agent. The measurements were performed in triplicates. Tumor and normal breast tissue from six patients were used for the assay that had been classified for Her2 expression using IHC in a routine clinical laboratory. The Her2 status of patient tumors 2, 3, 4 and 5 were rated 3+ on a scale from 0 to 3+. Tumor samples 1 and 6 were judged as 0. Using bead-based assays, Her2 positive tumor tissues were measured with median fluorescence intensities (MFIs) > 1000 AU, whereas Her2 negative tumor tissue resulted in MFIs < 100 AU. Moreover, a basal Her2 expression was detected from normal tissue with MFIs < 150 AU.

(Figure 6(a)). The overall performance seemed to correlate with the affinities of the clones. H10-2-G3 proved to be the most sensitive DARPin and was capable of detecting Her2 ECD down to a concentration of 20 pg/ml (0.2 pM), which is comparable to commercial ELISA kits. The dynamic range of the assay covered more than three orders of magnitude. The capturing potential of the DARPin H10-2-G3 was further compared to the mAb trastuzumab, which was immobilized on a microsphere by NHS-ester chemistry. The sensitivity of this setup was comparable to the capturing potential of the DARPin H10-2-G3. However, trastuzumab showed some deviations from linearity at high Her2 concentrations, possibly because of its dimeric nature and the higher molecular weight. In addition, trastuzumab showed a more than fivefold higher background signal with the applied detection system than H10-2-G3.

The combination of H10-2-G3 as a capture molecule and the monoclonal mouse antibody sp185 as the detector was used in a sandwich assay to quantify Her2 expression in tumor lysates. Samples from mammary carcinomas and normal breast tissue that had been analyzed by immuno-histochemistry (IHC) in a routine clinical laboratory were used, performing the assay with only 1 μg of total protein per sample. Data from the bead-based assays explicitly show a distinction between Her2-expressing tumors and normal tissue. A clear correlation of the Her2 expression from the sandwich assay with the clinical data from IHC could be observed (Figure 6(b)).

Discussion

Using ribosome display with a combination of error-prone PCR and stringent off-rate selection, we generated the highest affinity DARPin described up to now, with a monovalent affinity of 90 pM. This affinity surpasses the high-affinity natural ankyrin repeat proteins, such as the mouse GA binding protein (GABP) β1 binding GABPα, which was described to bind with an affinity of 0.78 nM,[22] and IκBα, whose affinity lies in the low nanomolar range.[23] When comparing the affinity to the size of the interaction surface, the difference becomes even more obvious: while the selected DARPins accomplish the binding with only two repeat modules, most natural ankyrin repeat proteins involve several repeat modules in binding.[24] A high percentage of hydrophobic interactions were found in the putative selected interaction interface. These contacts can contribute much to the free energy of the interaction within a small interaction surface. Nevertheless, specificity is maintained.

The use of error-prone PCR for the affinity maturation of DARPins proved to be a powerful approach. The random mutation of framework residues produced a kink in the rigid backbone of the DARPin and thereby added some variability to the scaffold by increasing the diversity of molecular shapes. Many mutations that contribute to high affinity, when comparing H10-G3 to the wild-type framework or to H10-G5 are most likely not part of the binding interface. We think that these mutations lead to subtle changes in the overall conformation. These changes are fundamental for a tight adaptation of the structure to the target and therefore for highest affinities. Introducing random mutations in the whole gene, followed by stringent selection, might be a general

means to adapt the binding site to the target surface. In a very stable framework such as that of a DARPin, such adaptations by directed evolution are possible, since the favorable biophysical properties can still be maintained. In addition, structural and kinetic analysis of the binding revealed some insight into the dynamics of framework residues.

We propose that a sparsely population of a kinked conformation was stabilized by a framework mutation at position 52 in the evolved DARPins. This would also explain the unusually slow association rate constants of the non-affinity matured clone G3-HAVD, which did not contain a tyrosine residue at position 52. Since the association rate of the DARPin with its antigen is a bimolecular event that is directly proportional to changes in concentration, the presence of two conformations of one binding partner would directly lead to a decrease of the association rate constant. Mutation of histidine 52 to tyrosine, however, forces residue 52 to rotate into the putative binding pocket due to the larger size of the side-chain ring and the additional hydroxyl group, thereby inducing the putative active conformation, resulting in a dramatic increase of the association rate constant to the level typical for protein–protein interactions.[8] This particular conformation appears to be crucial when binding the epitope of the KEYL family, but not for the epitopes recognized by the other families, as the other k_{on} values are normal, with and without the Tyr52 mutation.

An unexpected finding of our affinity maturation was that, even though we used off-rate selection, proteins with improved on-rates were obtained. We believe, however, that a plausible, albeit purely speculative rationalization can be proposed. It is useful to consider the single point mutants of G3 (G3-D, G3-A, G3-AVD, G3-HAVD, Table 1), even though these clones have not actually been observed as intermediates in the selection, but have only been constructed afterwards to investigate the selection procedure. The "wild-type" H3-HAVD (with unmutated framework) has a K_D of only 288 nM and it would be easily out-competed at equilibrium by G3-AVD (K_D 10 nM), carrying the His52Tyr mutation, especially since it also equilibrates much faster. This mutant, the putative precursor of G3-2-H10, has a relatively fast off-rate of 4.1×10^{-3} s^{-1} and from this point on, the off-rate decreased (40-fold), whereas the on-rate increased only slightly (2.5-fold), as expected for a classical off-rate selection.

The affinity maturation did not influence the specificity of H10-2-G3. For this mutant as well as all other tested, still no cross-reactivity was observed, and competition with trastuzumab was seen for several clones. Also, fusion to phage λ pD and modification with biotin did not influence the beneficial behavior of H10-2-G3. In a sandwich-ELISA approach, similar sensitivities for Her2 were observed as with a commercial antibody such as trastuzumab. Compared to the antibody-based assay, H10-2-G3 showed a lower background.

The accumulated mutations destabilized the DARPin compared to the clones not carrying framework mutations. The still high stability and the unchanged expression properties of the evolved DARPins show that the DARPin scaffold is well suited to tolerate multiple mutations at framework positions in addition to the randomized residues. These favorable biophysical properties in combination with the exceptional affinity, selectivity and sensitivity data make DARPins such as clone H10-2-G3 ideal candidates for miniaturized and even multiplexed assay systems, useful tools for diagnostic tests on microarray platforms or candidates for further drug development.

Materials and Methods

Error-prone PCR

Error-prone PCR in the presence of dNTP analogues[25] was performed to generate second generation libraries of pools that were previously selected.[12] Therefore, the pools isolated after round six in this previous study were used as template for error-prone PCR. Several reactions were performed with different concentrations of the dNTP analogues dPTP (6-(deoxy-β-D-erythro-pentofuranosyl)-3,4-dihydro-8H-pyrimido- [4,5-c][1,2]oxazine-7-one-5′-triphosphate) and 8-oxo-dGTP (8-oxo-2′-deoxyguanosine-5′-triphosphate) ranging from 2.5 μM to 20 μM each. The amplification was performed in a 50 μl reaction in the presence of 0.25 μM primers, one unit of Vent polymerase exo minus (NEB), 5% DMSO, 1.5 mM $MgCl_2$ and 200 μM dNTPs. A total of 23 cycles of PCR were performed, and the mutational load was determined by sequencing to be 1.3–5.9 mutations per DARPin. The distribution of transitions and transversions was similar to published values.[13]

Ribosome display selection rounds

For selection experiments, biotinylated Her2 ECD was immobilized *via* neutravidin as described.[12] For ELISA and RIA experiments, 250–500 ng of Her2 ECD were directly coated to 96-well MaxiSorp polystyrene plates (Nunc) by overnight incubation at 4 °C in phosphate-buffered saline (PBS).

Ribosome display off-rate selections were performed as described.[12,15] Biotinylated Her2 ECD was added to the stopped translation reaction at a concentration of 0.7 nM and equilibrated by shaking overnight at 4 °C. Non-biotinylated Her2 ECD was added in 500-fold excess (350 nM). This mixture was kept under slow shaking at 4 °C for times ranging from 10 h up to 27 days.

Ternary complexes that were still bound to the biotinylated Her2 ECD were isolated using streptavidin-coated magnetic beads (Roche). For recovery, 60 μl (0.6 mg) beads were washed three times in WBT (50 mM Tris acetic acid (pH 7.5), 150 mM NaCl, 50 mM $Mg(CH_3COO^-)_2$, 0.05% Tween 20) and then blocked for 1 h in WBT plus 0.5% (w/v) BSA at room temperature. After adding the beads, the ribosomal complexes were allowed to bind by shaking for 30 min at 4 °C. The beads were then washed three times for 3 min and three times 15 min with WBT before elution.

Crude extract ELISA, protein expression and surface plasmon resonance spectroscopy

For affinity analysis of single clones, the selected pools were cloned into plasmid pQE30 (Qiagen) *via* BamHI and HindIII. Because of the very strong expression of the DARPins, the single stop codon on pQE30 is partially read over leading to a C-terminal extension bearing a cysteine, which made an additional purification step for crystallization necessary. This step could be circumvented in the future by using a vector with two stop codons in tandem ($pQE30_{SS}$) (D.S. *et al.*, unpublished). Crude extract ELISAs were performed as described earlier[11] from lysates of 1 ml expression cultures. For SPR analysis, the DARPins were expressed in *E. coli* strain XL1-blue in 500 ml scale and purified over immobilized metal-ion affinity chromatography (IMAC) on a Superflow NTA matrix (Qiagen) as described.[11]

All SPR measurements were performed using a Biacore 3000 (Biacore). A CM5 chip was prepared according to the manufacturer's protocol. For the immobilization of neutravidin, a solution of 50 μg/ml neutravidin in 10 mM sodium acetate, 125 mM NaCl (pH 4.5) was used. Biotinylated Her2 ECD was then immobilized on the neutravidin-modified flow cells. For kinetic measurements, a chip was coated with 220 RU of biotinylated Her2 and for inhibition measurements with 2500 RU.

Kinetic measurements were performed by the serial injection of a DARPin in concentrations ranging from 1 nM to 250 nM at a buffer-flow of 30 μl/min in HBST (20 mM Hepes (pH 7.4), 150 mM NaCl, 0.05% Tween 20). Inhibition measurements were done as described[3] at a constant concentration of DARPin of 5 nM and different concentrations of soluble Her2 ECD as a competitor in concentrations ranging from 50 pM to 20 nM. The slope of the binding to a high-density chip was monitored in the linear range as a function of the concentration of competitor at a flow of 25 μl/min. Data evaluation was performed using BIAEVAL (Biacore), CLAMP[26] and SigmaPlot (Systat Software) as described.[16]

Construction of point mutants

To study the influence of the four framework mutations of H10-2-G3, several clones were constructed where one or more of these mutations were changed back to the consensus sequence. The following variants were constructed: G3-D (without mutation D122G), G3-A (without A55T), G3-AVD (without A55T, V96A, D122G) and G3-HAVD (without A55T, V96A, D122G, V96A, which corresponds to H10-2-G3 having no framework mutations).

The mutations were introduced by a PCR-based approach. Two fragments were amplified overlapping in the region of the desired mutation. In a second PCR reaction with outer primers only, the fragments were joined to yield the mutated sequence. Clone G3-D was constructed with a single PCR reaction using a long reverse primer, as the mutation was near to the C terminus. DNA of all clones was isolated from agarose gels and cloned *via* BamHI and HindIII into pQE-30 (Qiagen). Plasmids were prepared, sequenced and the mass of the expressed and purified clones was verified with mass spectrometry (MALDI-TOF).

Protein crystallization and X-ray data collection

Prior to crystallization, protease inhibitors and oligomeric protein species were removed from the protein solution by size-exclusion chromatography on a Superdex 200 10/30 column. Eluted protein was concentrated to 6 mg/ml using a Millipore Centricon 3 kDa centrifugal concentrator in 20 mM sodium phosphate (pH 7.4), 75 mM NaCl.

An initial screen of 808 commercial and in-house conditions was performed using a Cartesian Honeybee robot (Genomic Solutions, Michigan) to set up 96-well round-bottomed plates (Greiner, Germany) with 100 μl screening solution per well, 100 nl protein plus 100 nl well solution in the drops. The screen gave several leads, which were scaled up using protein at 10 mg/ml and optimized manually in hanging drops (24 well Linbro plates, 1 ml of solution per well, 1 μl protein plus 1 μl of well solution in drops, at room temperature). Crystals grew within three weeks from a solution containing 0.1 M Tris-HCl (pH 8.5), 2.3 M $(NH_4)_2SO_4$, 10% (v/v) glycerol. The crystal used for data collection exhibited a trapezoidal plate-like morphology, ca 0.25 mm × 0.08 mm × 0.15 mm.

A single crystal of the H10-2-G3 DARPin molecule was transferred to a cryo-protectant solution containing 2.3 M $(NH_4)_2SO_4$, 20% glycerol, 0.1 M Tris-HCl (pH 8.5) and mounted at −160 °C in a rayon loop[27] on a RU-3R X-ray generator (RigakuMSC, Texas) equipped with monocapillary focusing optics (AXCO, Australia). The crystal diffracted to at least 1.7 Å resolution. Two X-ray diffraction data sets were collected using the oscillation method; the first data set was collected with the camera set at $2\theta = 0°$ and the second at $2\theta = 15°$. Both data sets were processed using the software HKL.[28] The space-group of the crystal was *C*2 with unit cell dimensions $a = 152.40$ Å, $b = 51.97$ Å, $c = 70.07$ Å, $\beta = 105.21°$. X-ray data collection and processing statistics are presented in Table 2. We note that the R_{merge} statistics is high in the outer resolution shells of both data sets, however, the $\langle I \rangle / \langle s \rangle$, completeness and data redundancy statistics in this shell were judged satisfactory and these data were thus retained.

Structure determination and analysis

A molecular model encompassing 123 residues of the protein of an N2C DARPin, constructed from the two previously solved structures of N3C DARPins, E3_5 and E3_19 (with no framework mutations) was used for the molecular replacement search, employing the first diffraction data set and the program MOLREP[29] within the CCP4 suite.[30] Three copies of the search molecule (subsequently labelled A, B and C) were located within the asymmetric unit. The structure factor phases obtained by molecular replacement were then further improved using the program RESOLVE[31] and an atomic model built using the automated model-building procedure within that program. The atomic model was further improved by iterative cycles of crystallographic refinement against the second diffraction data set using REFMAC5[32] within the CCP4 suite and manual model building using O.[33] The final atomic model encompassed residues A12 to A135, B12 to B135 and C12 to C136 and included 488 ordered solvent molecules. Crystallographic refinement included a bulk solvent model, refinement of restrained individual atomic temperature factors and the refinement of individual TLS parameters[34] for the three monomers. Crystallographic refinement statistics are presented in Table 3. The structure was analyzed using the programs MolMol[35] and Swiss PDB viewer.

Structural comparison with N3C ankyrins

Each of the three copies of H10-2-G3 in the crystallographic asymmetric unit was overlaid using the pro-

Table 3. Crystallographic refinement statistics

Resolution range (Å)	15.0–1.7
No. of reflections in working set	53,757 (3768)
No. of reflections in free set	2929 (188)
R_{cryst} [a]	0.178 (0.287)
R_{free}	0.212 (0.395)
RMSD bond lengths (Å)	0.014
RMSD bond angles (°)	1.3
No. of protein atoms	2792
No. of solvent molecules	488
$<B>$ protein atoms (Å^2)	34.5
$<B>$ solvent molecules (Å^2)	38.9
Ramachadran plot details[36] (no. of residues)	
Most favored regions	299
Additional allowed region	26
Generously allowed region	0
Disallowed region	0

[a] $R_{cryst} = \sum_h | F_h^{obs} - k F_h^{calc} | / \sum_h | F_h^{obs} |$.

gram LSQMAN[36] onto the three N-terminal ankyrin repeats of three representative N3C structures extracted from the Protein Data Bank (entries 2BBK, 1MJ0 and 1SVX). Analysis of the resultant geometric transformations was conducted manually, whilst analysis of relative changes in the hydrogen bonding patterns was conducted using HBPLUS.[37]

Thermal denaturation

Thermal denaturation experiments were performed and evaluated as described.[11] Briefly, 15 μM purified protein in PBS were brought from 20 °C to 92 °C with a heating rate of 0.5 deg./min and the CD signal at 222 nm was recorded. Data were recorded with a Jasco J-715 instrument.

Sensitivity analysis of selected DARPins in Luminex assays

Biotinylated DARPins H10-2-A2, H10-2-D11, H10-2-G3, H10-2-G11 and DARPin H6-3-B3, which is an N3C DARPin that has been described earlier[12] were expressed with the N-terminal fusion protein avi-pD by cloning into vector pAT224 (GenBank accession number AY327139) and purified as described above. By co-expression with BirA, the biotin ligase of *E. coli*, the DARPins could be biotinylated site-specifically *in vivo* as described earlier.[11]

Each sample was immobilized on Luminex beads of distinguishable color-code according to the manufacturer's protocol (Luminex-Corp., Austin, Tx, USA). Biotinylated DARPins were immobilized on avidin-coated beads (LumAvidin Microspheres). Trastuzumab was coupled to carboxylated beads (COOH Microspheres). A recombinant Her2 ECD (BenderMed Systems, Vienna, Austria) served as antigen in sandwich-ELISA set-up. Breast cancer tumor tissue and corresponding normal tissue were kindly provided by Helmut Deissler (University of Ulm, Medical School, Germany). All tissue samples were solubilized as described.[38] The total amount of protein was determined by the Bradford assay.

Immobilized DARPins were studied in multiplexed sandwich immunoassays to compare capture activities for quantitative Her2 analysis. All assays were performed in Blocking Reagent for ELISA (Roche) with 0.005% Tween at pH 7.4 under permanent shaking in microtiter plates. Six differently color-coded Luminex beads, each loaded with a different DARPin or trastuzumab, were mixed. Titration series of recombinant Her2 protein or tissue samples were incubated with the bead mixture in a volume of 50 μl overnight at 4 °C. After filtering the assay mixture in a 96-well filter plate (Pall, East Hills, NY, USA) the beads were resuspended in 30 μl of assay buffer containing 1 μg/ml of anti-Her2 antibody sp185 (BenderMed Systems) and incubated for 60 min. Bound antibody was detected using R-phycoerythrin (R-PE) labeled, Fc fragment-specific goat anti-mouse antibody (Dianova, Hamburg, Germany) at a concentration of 2.5 μg/ml over 45 min incubation. The beads were analyzed in a Luminex 100 IS System. Results are presented as median fluorescence intensity (MFI) of 100 events counted per bead population.

Protein Data Bank accession code

Atomic coordinates for the high affinity DARPin have been deposited in the PDB under accession code 2jab.

Acknowledgements

We thank Helmut Deissler from the University of Ulm, Germany, for kindly providing breast cancer tissues. We further thank Thomas Huber for his help and valuable discussions in data evaluation. This work was supported by a grant from the Swiss National Center of Competence in Research in Structural Biology.

Supplementary Data

Supplementary data associated with this article can be found, in the online version, at doi:10.1016/j.jmb.2007.03.028

References

1. Allen, T. M. (2002). Ligand-targeted therapeutics in anticancer therapy. *Nature Rev. Cancer*, **2**, 750–763.
2. Moroney, S. & Plückthun, A. (2005). Modern antibody technology: the impact on drug development. In *Modern Biopharmaceuticals* (Knäblein, J. & Müller, R. H., eds), pp. 1147–1185, WILEY-VCH Verlag GmbH & Co. KGaA, Weinheim.
3. Hanes, J. & Plückthun, A. (1997). In vitro selection and evolution of functional proteins by using ribosome display. *Proc. Natl Acad. Sci. USA*, **94**, 4937–4942.
4. Smith, G. P. (1985). Filamentous fusion phage: novel expression vectors that display cloned antigens on the virion surface. *Science*, **228**, 1315–1317.
5. Chen, Y., Wiesmann, C., Fuh, G., Li, B., Christinger, H. W., McKay, P. *et al.* (1999). Selection and analysis of an optimized anti-VEGF antibody: crystal structure of an affinity-matured Fab in complex with antigen. *J. Mol. Biol.* **293**, 865–881.
6. Jermutus, L., Honegger, A., Schwesinger, F., Hanes, J. & Plückthun, A. (2001). Tailoring in vitro evolution for protein affinity or stability. *Proc. Natl Acad. Sci. USA*, **98**, 75–80.
7. Zahnd, C., Spinelli, S., Luginbühl, B., Amstutz, P.,

Cambillau, C. & Plückthun, A. (2004). Directed in vitro evolution and crystallographic analysis of a peptide-binding single chain antibody fragment (scFv) with low picomolar affinity. *J. Biol. Chem.* **279**, 18870–18877.
8. Northrup, S. H. & Erickson, H. P. (1992). Kinetics of protein-protein association explained by Brownian dynamics computer simulation. *Proc. Natl Acad. Sci. USA*, **89**, 3338–3342.
9. Binz, H. K., Stumpp, M. T., Forrer, P., Amstutz, P. & Plückthun, A. (2003). Designing repeat proteins: well-expressed, soluble and stable proteins from combinatorial libraries of consensus ankyrin repeat proteins. *J. Mol. Biol.* **332**, 489–503.
10. Forrer, P., Binz, H. K., Stumpp, M. T. & Plückthun, A. (2004). Consensus design of repeat proteins. *ChemBioChem.* **5**, 183–189.
11. Binz, H. K., Amstutz, P., Kohl, A., Stumpp, M. T., Briand, C., Forrer, P. *et al.* (2004). High-affinity binders selected from designed ankyrin repeat protein libraries. *Nature Biotechnol.* **22**, 575–582.
12. Zahnd, C., Pecorari, F., Straumann, N., Wyler, E. & Plückthun, A. (2006). Selection and characterization of Her2-binding designed ankyrin repeat proteins. *J. Biol. Chem.* **281**, 35167–35175.
13. Zaccolo, M. & Gherardi, E. (1999). The effect of high-frequency random mutagenesis on in vitro protein evolution: a study on TEM-1 beta-lactamase. *J. Mol. Biol.* **285**, 775–783.
14. Karlsson, R. (1994). Real-time competitive kinetic analysis of interactions between low- molecular-weight ligands in solution and surface-immobilized receptors. *Anal. Biochem.* **221**, 142–151.
15. Nieba, L., Krebber, A. & Plückthun, A. (1996). Competition BIAcore for measuring true affinities: large differences from values determined from binding kinetics. *Anal. Biochem.* **234**, 155–165.
16. Hanes, J., Jermutus, L., Weber-Bornhauser, S., Bosshard, H. R. & Plückthun, A. (1998). Ribosome display efficiently selects and evolves high-affinity antibodies in vitro from immune libraries. *Proc. Natl Acad. Sci. USA*, **95**, 14130–14150.
17. Lovell, S. C., Word, J. M., Richardson, J. S. & Richardson, D. C. (2000). The penultimate rotamer library. *Proteins: Struct. Funct. Genet.* **40**, 389–408.
18. Kohl, A., Binz, H. K., Forrer, P., Stumpp, M. T., Plückthun, A. & Grütter, M. G. (2003). Designed to be stable: crystal structure of a consensus ankyrin repeat protein. *Proc. Natl Acad. Sci. USA*, **100**, 1700–1705.
19. Mosavi, L. K., Williams, S. & Peng Zy, Z. Y. (2002). Equilibrium folding and stability of myotrophin: a model ankyrin repeat protein. *J. Mol. Biol.* **320**, 165–170.
20. Cho, H. S., Mason, K., Ramyar, K. X., Stanley, A. M., Gabelli, S. B., Denney, D. W., Jr & Leahy, D. J. (2003). Structure of the extracellular region of HER2 alone and in complex with the Herceptin Fab. *Nature*, **421**, 756–760.
21. Franklin, M. C., Carey, K. D., Vajdos, F. F., Leahy, D. J., de Vos, A. M. & Sliwkowski, M. X. (2004). Insights into ErbB signaling from the structure of the ErbB2-pertuzumab complex. *Cancer Cell*, **5**, 317–328.
22. Suzuki, F., Goto, M., Sawa, C., Ito, S., Watanabe, H., Sawada, J. & Handa, H. (1998). Functional interactions of transcription factor human GA-binding protein subunits. *J. Biol. Chem.* **273**, 29302–29308.
23. Malek, S., Huxford, T. & Ghosh, G. (1998). IκBα functions through direct contacts with the nuclear localization signals and the DNA binding sequences of NF-κB. *J. Biol. Chem.* **273**, 25427–25435.
24. Mosavi, L. K., Cammett, T. J., Desrosiers, D. C. & Peng, Z. Y. (2004). The ankyrin repeat as molecular architecture for protein recognition. *Protein Sci.* **13**, 1435–1448.
25. Zaccolo, M., Williams, D. M., Brown, D. M. & Gherardi, E. (1996). An approach to random mutagenesis of DNA using mixtures of triphosphate derivatives of nucleoside analogues. *J. Mol. Biol.* **255**, 589–603.
26. Myszka, D. G. & Morton, T. A. (1998). CLAMP: a biosensor kinetic data analysis program. *Trends Biochem. Sci.* **23**, 149–150.
27. Teng, T. Y. (1990). Mounting of crystal for macromolecular crystallography in a free standing thin film. *J. Appl. Crystallog.* **23**, 387–391.
28. Otwinowski, Z. & Minor, W. (1997). Processing of X-ray diffraction data collected in oscillation mode. *Methods Enzymol.* **276**, 307–326.
29. Vagin, A. & Teplyakov, A. (1997). MOLREP: an automated program for molecular replacement. *J. Appl. Crystallog.* **30**, 1022–1025.
30. CCP4. (1994). The CCP4 Suite: programs for protein crystallography. *Acta Crystallog. sect. D*, **50**, 760–763.
31. Terwilliger, T. (2004). SOLVE and RESOLVE: automated structure solution, density modification and model building. *J. Synchrotron Radiat.* **11**, 49–52.
32. Murshudov, G. N., Alexei, A. V. & Dodson, E. J. (1997). Refinement of macromolecular structures by the maximum-likelihood method. *Acta Crystallog. sect. D*, **53**, 240–255.
33. Jones, T. A., Zou, J. Y., Cowan, S. W. & Kjeldgaard (1991). Improved methods for building protein models in electron density maps and the location of errors in these models. *Acta Crystallog. sect. A*, **47**, 110–119.
34. Winn, M. D., Isupov, M. N. & Murshudov, G. N. (2001). Use of TLS parameters to model anisotropic displacements in macromolecular refinement. *Acta Crystallog. sect. D*, **57**, 122–133.
35. Koradi, R., Billeter, M. & Wüthrich, K. (1996). MOLMOL: a program for display and analysis of macromolecular structures. *J. Mol. Graph.* **14**, 51–5, 29–32.
36. Kleywegt, G. J. & Jones, T. A. (1994). A super position. *CCP4/ESF-EACBM News. Protein Crystallog.* **31**, 9–14.
37. McDonald, I. K. & Thornton, J. M. (1994). Satisfying hydrogen bonding potential in proteins. *J. Mol. Biol.* **238**, 777–793.
38. Schneiderhan-Marra, N., Kirn, A., Döttinger, A., Templin, M. F., Sauer, G., Deissler, H. & Joos, T. O. (2005). Protein microarrays - a promising diagnostic tool for cancer. *Cancer Genomics Proteomics*, **2**, 37–42.
39. Fenn, T. D., Ringe, D. & Petsko, G. A. (2003). POVScript+: a program for model and data visualization using persistence of vision ray-tracing. *J. Appl. Crystallog.* **36**, 944–947.

Edited by I. Wilson

(Received 13 July 2006; received in revised form 10 March 2007; accepted 13 March 2007)
Available online 20 March 2007